JCB Article

Discovery of a novel murine keratin 6 (K6) isoform explains the absence of hair and nail defects in mice deficient for K6a and K6b

Sonja M. Wojcik,[1] Mary A. Longley,[1] and Dennis R. Roop[1,2]

[1]Department of Molecular and Cellular Biology and [2]Department of Dermatology, Baylor College of Medicine, Houston, TX 77030

The murine genome is known to have two keratin 6 (K6) genes, mouse K6 (MK6)a and MK6b. These genes display a complex expression pattern with constitutive expression in the epithelia of oral mucosa, hair follicles, and nail beds. We generated mice deficient for both genes through embryonic stem cell technology. The majority of MK6a/b$^{-/-}$ mice die of starvation within the first two weeks of life. This is due to a localized disintegration of the dorsal tongue epithelium, which results in the build up of a plaque of cell debris that severely impairs feeding. However, ~25% of MK6a/b$^{-/-}$ mice survive to adulthood. Remarkably, the surviving MK6a/b$^{-/-}$ mice have normal hair and nails. To our surprise, we discovered MK6 staining both in the hair follicle and the nail bed of MK6a/b$^{-/-}$ mice, indicating the presence of a third MK6 gene. We cloned this previously unknown murine keratin gene and found it to be highly homologous to human K6hf, which is expressed in hair follicles. We therefore termed this gene MK6 hair follicle (MK6hf). The presence of MK6hf in the MK6a/b$^{-/-}$ follicles and nails offers an explanation for the absence of hair and nail defects in MK6a/b$^{-/-}$ animals.

Introduction

Keratins are cytoskeletal proteins that form the intermediate filament (IF)* network of epithelial cells. Keratin 6 (K6) expression, which has been described for humans, mice, and bovines, is characteristically seen in hair follicles, oral epithelia, nail bed, and palmoplantar epidermis. In addition to this constitutive expression, K6 is induced in the epidermis in response to wounding. Since keratin IFs (KIFs) assemble from heterodimers made up of one type I and one type II keratin (Hatzfeld and Weber, 1990; Steinert, 1990), keratins are generally considered to be coexpressed with specific partners of the opposite type. K6, a type II keratin, is thought to have two type I partners, K16 and K17, because they exhibit an expression pattern similar to that of K6 and are also induced in the epidermis in response to wounding. K6, K16, and K17 are also induced in certain skin diseases that exhibit keratinocyte hyperproliferation, such as psoriasis, and are therefore frequently described as hyperproliferation- or activation-associated keratins (Jiang et al., 1993; Leigh et al., 1995). However, the biological significance of their induction is not well understood. A feature that appears to be unique to K6 is that several active genes have been described in humans, mice, and bovines. Mice are known to have two closely related isoforms, mouse K6 (MK6)a and MK6b (termed MK6α and MK6β by Takahashi and colleagues; Takahashi et al., 1998; Rothnagel et al., 1999); humans may have as many as seven active human K6 (HK6) isoforms, HK6a through HK6f (Takahashi et al., 1995), as well as HK6 hair follicle (HK6hf) (Winter et al., 1998). The gene number in bovines has not been fully investigated, but there may be as many as three active genes (Blessing et al., 1987; Navarro et al., 1995). The MK6a and MK6b genes are highly homologous and are separated by ~10.5–13 kb of intergenic DNA (Takahashi et al., 1998; Rothnagel et al., 1999). In addition to MK6a and MK6b, mice have at least two K6 pseudogenes (Takahashi et al., 1998).

Mutations in keratins underlie several inherited skin fragility syndromes. These are largely dominant-negative mutations, leading to the collapse of the KIFs in cells expressing the mutant keratin (for review see Corden and McLean, 1996). To date, mutations in two HK6 genes and also in HK16 and HK17 have been described as the underlying cause of two hereditary disorders, which share a characteris-

Address correspondence to Dennis R. Roop, Department of Molecular and Cellular Biology, Baylor College of Medicine, 1 Baylor Plaza, Houston, TX 77030. Tel.: (713) 798-4966. Fax: (713) 798-3800. E-mail: roopd@bcm.tmc.edu

*Abbreviations used in this paper: ES, embryonic stem; HK6, human K6; HK6hf, HK6 hair follicle; IF, intermediate filament; K6, keratin 6; KIF, keratin IF; MK6, mouse K6; MK6hf, MK6 hair follicle; ORS, outer root sheath; PC, pachyonychia congenita; RACE, rapid amplification of cDNA ends.

Key words: keratin; skin; tongue; hair follicle; pachyonychia congenita

tic thickening of the nail and nail bed and are therefore named pachyonychia congenita (PC) type 1 and type 2. Mutations in HK6a and HK16 have been found in patients with PC-1 (Bowden et al., 1995; McLean et al., 1995; Smith et al., 1999a,b,c) who show abnormalities of nails, palmar and plantar surfaces as well as the tongue epithelium, whereas mutations in HK6b and HK17 have been reported in PC-2 patients (McLean et al., 1995; Fujimoto et al., 1998; Smith et al., 1998; Celebi et al., 1999), who lack oral involvement but have follicular and nail abnormalities. Steatocystoma multiplex and nonepidermolytic palmoplantar keratoderma are two additional disorders in which mutations in HK17 and HK16, respectively, have been identified (Shamsher et al., 1995; Covello et al., 1998).

In hair follicles, K6 and K16 are constitutively expressed in the innermost cell layer of the outer root sheath (ORS) (Takahashi et al., 1998; Winter et al., 1998; Rothnagel et al., 1999). This single cell layer is also known as the companion cell layer and consists of highly specialized elongated cells (Ito, 1986, 1988; Orwin, 1971). Since we have previously shown that expression of mutant MK6a transgenes leads to a complete destruction of these cells followed by hair loss (Wojcik et al., 1999), it may seem surprising that the hair abnormalities in PC-2 patients with HK6b mutations are very mild. However, unlike MK6a and MK6b, which are expressed in the companion cells, HK6b expression in the hair follicles was shown to be restricted to the sebaceous glands (Smith et al., 1998). In humans, only HK6hf, in which no mutations have been described, has conclusively been shown to be expressed in the companion cell layer (Winter et al., 1998).

To investigate the function of K6, we had previously generated MK6a$^{-/-}$ mice. Unlike the majority of other keratin knockout mice (Lloyd et al., 1995; Kao et al., 1996; Porter et al., 1996; Ness et al., 1998), these mice exhibited no signs of epithelial fragility, but displayed a delay in reepithelialization of superficial wounds from the hair follicles, whereas the healing of full thickness wounds was normal (Wojcik et al., 2000). At the time we attributed the lack of structural defects in the companion cell layer, oral epithelia and nails to the presence of MK6b in these compartments. However, it now appears that this assumption was only correct with respect to the oral epithelia. Since our MK6a$^{-/-}$ mice exhibited only a mild wound healing phenotype but no structural defects, we generated MK6a/b$^{-/-}$ mice. We found that the majority of our MK6a/b$^{-/-}$ pups developed oral lesions, which led to starvation and death. However, ~25% of MK6a/b$^{-/-}$ mice survived to adulthood. Remarkably, the adult MK6a/b$^{-/-}$ survivors had normal hair and normal nails. To our surprise, we discovered strong reactivity with two separate K6 antibodies both in the companion cell layer and in the nail bed of MK6a/b$^{-/-}$ mice, indicating the existence of a third MK6-like gene. When we cloned the cDNA of this novel murine keratin gene, we found it to be highly homologous to HK6hf and therefore named it MK6 hair follicle (MK6hf). Since MK6hf is not expressed in oral epithelia, it does not explain the survival of some of the MK6a/b$^{-/-}$ mice. However, the existence of the MK6hf isoform may be the explanation for the otherwise somewhat puzzling absence of nail and hair defects in the MK6a/b$^{-/-}$ mice.

Results

Deletion of MK6a and MK6b from the genome

The MK6a/b targeting vector was designed to delete the complete coding regions of the MK6a and MK6b genes as well as the intervening 10.5 kb, resulting in a deletion of ~18 kb (Fig. 1 a). The targeting vector was introduced into 129/SvEv AB2.2 embryonic stem (ES) cells. Successfully targeted clones were confirmed by Southern analysis using 5′ and 3′ external probes (Fig. 1 b). Targeted clones were injected into C57BL/6N blastocysts, and the chimeras were bred to C57BL/6N females. Germline transmission was obtained from one clone, and the first F1 MK6a/b$^{+/-}$ males were crossed with wild-type C57BL/6N females. The resulting MK6a/b$^{+/-}$ F2 animals were intercrossed, and their offspring were used for all analyses performed in this study. The absence of MK6a and MK6b transcripts was confirmed by RNase protection analysis (Fig. 1 d).

Postnatal mortality in MK6a/b$^{-/-}$ mice due to oral hyperplastic lesions

Litters from the first MK6a/b$^{+/-}$ crosses were genotyped shortly after birth (Fig. 1 c), and MK6a/b$^{+/+}$, MK6a/b$^{+/-}$, and MK6a/b$^{-/-}$ animals were found at the expected Mendelian frequencies. However, the majority (~75%) of MK6a/b$^{-/-}$ mice subsequently failed to thrive, which became apparent at different times in different animals. The majority of MK6a/b$^{-/-}$ pups began to lag behind in their growth when compared with the MK6a/b$^{+/+}$ and MK6a/b$^{+/-}$ littermates between the ages of 3 and 7 d after birth. Such pups progressively became more emaciated over the course of 3–5 d and ultimately died of apparent starvation, usually before they reached 2 wk of age. Shown are a MK6a/b$^{-/-}$ pup and a MK6a/b$^{+/+}$ pup at 8 d of age (Fig. 2 a). However, some MK6a/b$^{-/-}$ animals were outwardly indistinguishable from their MK6a/b$^{+/+}$ and MK6a/b$^{+/-}$ littermates and survived to adulthood. Out of 109 pups that were genotyped after weaning, 70 were heterozygotes, 30 wild type, and 9 were surviving knockouts. Since we had previously found a normal Mendelian distribution of MK6a/b$^{+/-}$, MK6a/b$^{+/+}$, and MK6a/b$^{-/-}$ genotypes in litters screened immediately after birth, we estimated, based on the numbers shown above, the survival rate of MK6a/b$^{-/-}$ animals to be 27%. The surviving MK6a/b$^{-/-}$ animals reached normal adult size and were fertile. Matings of MK6a/b$^{-/-}$ animals produced litters with survival rates that varied between litters and ranged from 50–100%. This strongly suggests a genetic, rather than environmental reason for the survival of some of the MK6a/b$^{-/-}$ animals.

To determine the cause of death, MK6a/b$^{-/-}$ pups that showed signs of starvation as well as MK6a/b$^{+/-}$ littermates were killed at days 4, 8, and 10 after birth. Dissection of the heads revealed a macroscopically visible thickening, confined to the center of the very back of the dorsal tongue in the MK6a/b$^{-/-}$ animals (Fig. 2 c), whereas wild-type and heterozygote tongues were smooth (Fig. 2 b). Histological analysis of the oral cavity revealed that this thickening consisted of a plaque of amorphous material, which appeared to be cellular debris (Fig. 2 e). The plaque on the tongue was large enough to fill the back of the oral cavity. The back of the oral cavity of a wild-type littermate is shown for compar-

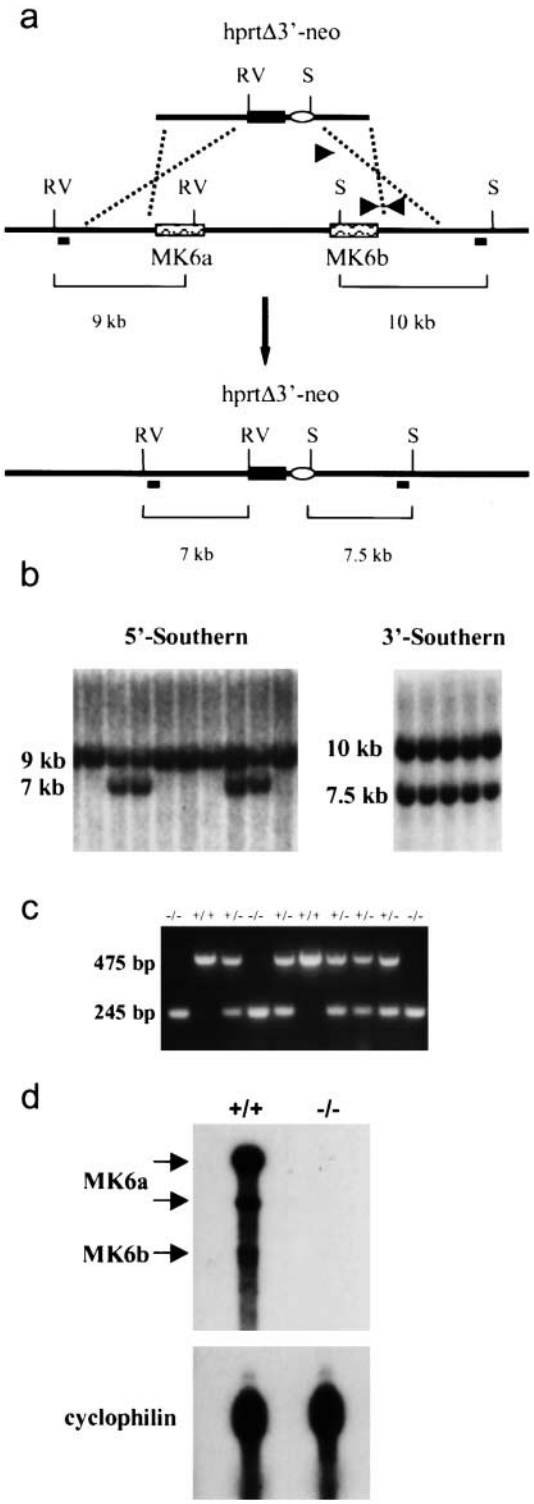

Figure 1. **Targeting of MK6a and MK6b.** (a) A replacement vector containing the hprtΔ3′-neo cassette was used to delete MK6a, MK6b, and the intergenic region. The positions of the 5′ and 3′ external probes are indicated by short bars. The triangles indicate the position of the PCR primers used for genotyping. (b) Genomic Southerns: 5′ Southern, EcoRV (RV) digest, showing the wild-type 9-kb and the targeted 7-kb fragments detected with the 5′ external probe; 3′ Southern, SphI (S) digest, showing the 10-kb wild-type and 7.5-kb targeted allele. (c) Genomic PCR of the 3′ end of the targeted locus showing a 475-bp product for the MK6a/b$^{+/+}$ genotype, a 245-bp product for MK6a/b$^{-/-}$, and both fragments for MK6a/b$^{+/-}$. (d) RNase protection assay of RNA isolated from uninduced skin with anagen hair follicles. Both MK6a and MK6b mRNAs are absent in the MK6a/b$^{-/-}$ sample. The probe was designed to protect 382 bases in MK6a and 268 bases in MK6b. Please note that two bands are generated for the MK6a transcript, most likely due to a polymorphism present in the C57BL6/N strain, resulting in partial degradation of the 382-bp fragment. A cyclophilin probe was used as a loading control.

ison (Fig. 2 d). Furthermore, the palate epithelium opposing the plaque on the tongue showed a similar albeit smaller plaque. Examination at higher magnification revealed that at the transition between tongue epithelium and plaque, the epithelial cells appeared to be losing their nuclei, whereas the cell remnants remained attached to each other (Fig. 2 g). The intact papillae from the tongue of a wild-type littermate are shown for comparison (Fig. 2 f). The plaque was restricted to the back and center of the tongue and palate, whereas the rest of the tongue and palate epithelium was normal in appearance. The plaque was found in all MK6a/b$^{-/-}$ animals that either died of apparent starvation or were killed because of their emaciated appearance. Experimental removal of plaque material from the oral cavity of live pups led to a temporary weight gain, but the plaque size increased again and the animals ultimately died. Surprisingly, when we killed pups of MK6a/b$^{-/-}$ crosses that showed no signs of starvation at approximately 1 wk of age, we also found small plaques on their tongues. Except for their smaller size these plaques were microscopically identical to the ones found in starving pups (not shown). This suggests that all MK6a/b$^{-/-}$ pups develop plaques, but in some animals these resolve (see below), allowing those animals to survive.

Immunofluorescence analysis of MK6a/b$^{-/-}$ animals showed the complete absence of MK6 staining in tongue and palate (Fig. 2, i and k). MK16 staining in MK6a/b$^{-/-}$ animals appeared unaltered by immunofluorescence analysis. We had previously determined that MK6b expression in tongue, as in other epithelia, is suprabasal, and shown that one of our K6 antibodies recognizes MK6b, but not MK6a (Wojcik et al., 2000). Interestingly, examination of the staining pattern for MK6b and MK16 along the length of the tongue in MK6a/b$^{+/+}$ animals showed that both MK6b and MK16 staining became more widespread throughout the dorsal tongue epithelium towards the back of the tongue (Fig. 2, h and j). In the front and middle of the tongue MK16 staining was restricted to the papillae and MK6b staining to the very tips of the papillae in wild-type mice (Fig. 2 h). In the posterior half of the tongue, where the lesions occur in MK6a/b$^{-/-}$ animals (Fig. 2 k), MK16 was present throughout the tongue epithelium and MK6b staining was seen throughout the papillae of MK6a/b$^{+/+}$ samples (Fig. 2 j). The fact that MK6b expression is the highest in the back of the tongue could indicate that this area is subjected to the most mechanical stress and could serve as an explanation as to why the lesions in MK6a/b$^{-/-}$ mice occur in this region.

The tongues of surviving MK6a/b$^{-/-}$ mice are macroscopically normal but show slight alterations of the lingual papillae

To determine if surviving adult MK6a/b$^{-/-}$ animals showed any sign of a plaque, several MK6a/b$^{-/-}$ adults were killed

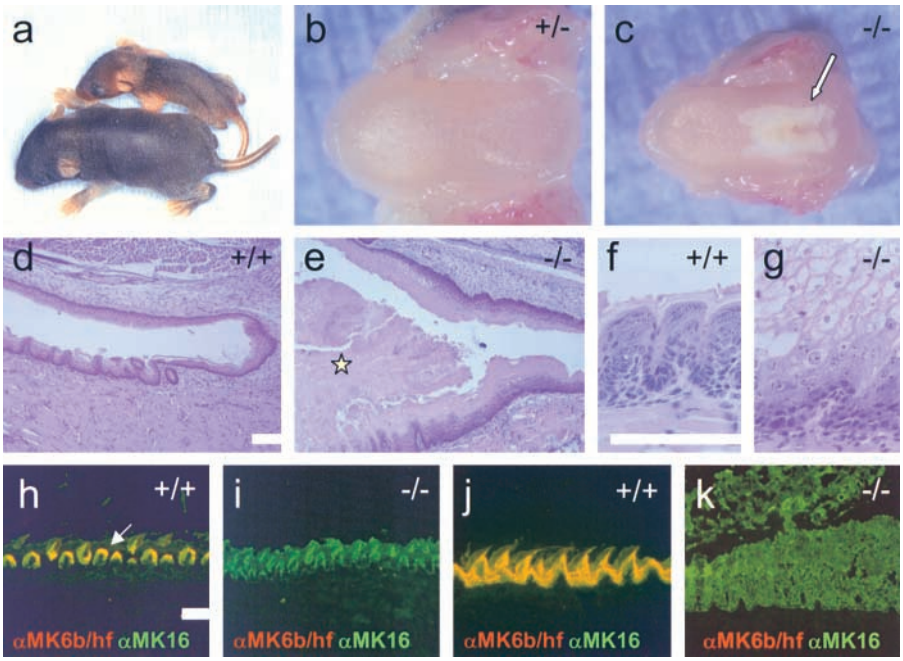

Figure 2. **Oral lesions in MK6a/b$^{-/-}$ mice occur in the back of the oral cavity where MK6b expression in the tongue is highest in wild-type animals.** (a) MK6a/b$^{-/-}$ pup (top) at 8 d showing signs of starvation. A wild-type littermate is shown for comparison. (b) Lower jaw of 8-d-old MK6a/b$^{+/-}$ pup. The tongue appears smooth. (c) Lower jaw of 8-d-old MK6a/b$^{-/-}$ pup. Note the white plaque in the back and center of the tongue (arrow). (d) MK6a/b$^{+/+}$ tongue and palate in the back of the oral cavity of 10-d-old pup. (e) MK6a/b$^{-/-}$ tongue and palate in the back of the oral cavity of 10-d-old pup, showing plaque formation on the tongue and palate epithelium. Note that the plaque on the tongue (☆) fills almost the entire oral cavity. (f) MK6a/b$^{+/+}$ tongue epithelium at high magnification showing the appearance of the papillae from the back of the tongue. (g) MK6a/b$^{-/-}$ tongue epithelium at high magnification showing that the plaque is composed of cell remnants that remain attached to each other. Note that the superficial cells of the papillae appear to be losing their cytoplasmic content and nuclei. (h–k) Images stained with MK6b/hf (red) and MK16 (green) antibodies; areas with overlapping staining appear yellow. (h) MK6a/b$^{+/+}$, note that in the middle of the tongue MK6b is restricted to the uppermost cells of the papillae (arrow). (i) The middle of the MK6a/b$^{-/-}$ tongue epithelium appears intact in spite of the absence of MK6. (j) MK6a/b$^{+/+}$, note that in the back of the tongue MK6b is expressed throughout the papillae. (k) MK6a/b$^{-/-}$ lesion in the back of the tongue epithelium, which corresponds to the site where MK6b expression is most widespread in wild-type tongue. Bars, 100 μm.

and their tongues were examined macroscopically, histologically, and ultrastructurally. The macroscopic appearance of the MK6a/b$^{-/-}$ survivor tongues was normal; they were smooth and indistinguishable from the tongues of age-matched wild-type mice (data not shown). However, histological examination revealed a subtle difference in the appearance of the papillae of the tongue of adult MK6a/b$^{-/-}$ survivors and wild-type littermates (Fig. 3, a and b). Mouse tongue epithelium possesses four distinct types of papillae (filiform, fungiform, foliate, and the single circumvallate papilla) (Paulson et al., 1985). The filiform papillae are by far the most numerous, and their highly ordered columns of cells make up the greater part of the dorsal lingual epithelium. Three alternating cell columns are easily distinguished from one another: the anterior column cells of the filiform papillae, the posterior column cells of the papillae, and the interpapillar cell columns. The anterior column cells contain keratohyalin granules and show a degree of keratinization similar to that of newborn skin (Iwasaki et al., 1999). The posterior column cells and interpapillary column cells contain no keratohyalin granules, and the latter show only weak keratinization. The most noticeable difference between MK6a/b$^{-/-}$ survivor (Fig. 3, b and d) and MK6a/b$^{+/+}$ tongues (Fig. 3, a and c) was an increase in thickness of the MK6a/b$^{-/-}$ tongue epithelium, including its keratinized layers. Furthermore, the anterior column cells, and to a lesser degree the posterior column cells of the MK6a/b$^{-/-}$ filiform papillae, appeared less tightly organized in their stacking (Fig. 3 d) when compared with the cells of wild-type papillae (Fig. 3 c). To determine if the apparent thickening of the MK6a/b$^{-/-}$ survivor tongues was due to an increase in proliferation, adult MK6a/b$^{-/-}$ survivors as well as heterozygous littermates were injected intraperitoneally with BrdU and killed after 1.5 h, and their tongues were examined for BrdU labeling by immunofluorescence analysis (Fig. 3, e and f). The MK6a/b$^{-/-}$ survivor tongues (Fig. 3 f) showed twofold higher BrdU labeling than the MK6a/b$^{+/-}$ tongues (Fig. 3 e), based on the averaged counts from four fields per section from four animals. This suggests that the tongue epithelium of MK6a/b$^{-/-}$ survivors responds to a slight structural defect with increased cell division.

MK6a/b$^{-/-}$ survivors show slight ultrastructural alterations in the lingual papillae, as opposed to a complete loss of papillary structure in the tongues of starving MK6a/b$^{-/-}$ mice with plaques

The alterations in the MK6a/b$^{-/-}$ survivor tongue epithelium that we observed at the histological level were confirmed by electron microscopy (Fig. 4). We took tongue samples from surviving MK6a/b$^{-/-}$ animals as well as from MK6a/b$^{-/-}$ pups whose tongues had a plaque, and from wild-type littermate controls. The overview of an adult filiform papilla in Fig. 4 a shows the tight organization of the keratohyalin granule-filled anterior column cells as well as some granule-free posterior column cells. Comparison of the anterior column cells of wild-type animals (Fig. 4 b) and MK6a/b$^{-/-}$ survivors (Fig. 4 c) shown at higher magnification confirms a slight disarray of the tightly stacked organization of these cells in the MK6a/b$^{-/-}$ survivors. Strikingly, whereas wild-type anterior column cells contain prominent KIF bundles (Fig. 4 b, inset), the MK6a/b$^{-/-}$ anterior column cells of both survivor tongues (Fig. 4 c) and tongues with plaques (Fig. 4 d, inset) are devoid of KIF bundles and

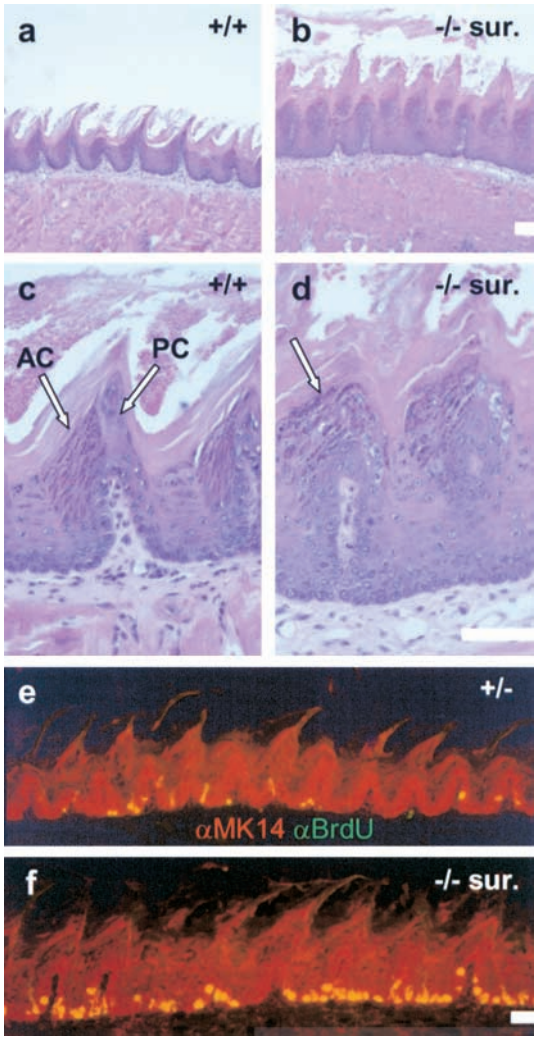

Figure 3. **Histological abnormalities and increased cell proliferation in MK6a/b$^{-/-}$ survivor tongue epithelium.** (a) MK6a/b$^{+/+}$ adult dorsal tongue epithelium, taken from the back of the tongue. (b) MK6a/b$^{-/-}$ adult survivor dorsal tongue epithelium, taken from the same region as in a. The MK6a/b$^{-/-}$ epithelium is noticeably thicker than the MK6a/b$^{+/+}$ epithelium. (c) MK6a/b$^{+/+}$ tongue epithelium at higher magnification showing the anterior column cells (AC) and the posterior column cells (PC) of the filiform papillae. Note the tightly stacked appearance of the cell columns. (d) MK6a/b$^{-/-}$ survivor tongue at the same magnification as c showing the disorganized appearance of the fililorm papillae, especially of the anterior column cells (arrow). (e) MK6a/b$^{+/-}$ dorsal tongue epithelium stained with an MK14 antibody (Texas red) and an BrdU antibody (FITC). (f) MK6a/b$^{-/-}$ survivor dorsal tongue epithelium stained with the same antibodies as in e. Bars, 50 μm.

instead contain what appear to be keratin clumps. However, in the MK6a/b$^{-/-}$ adult survivors, in spite of some structural abnormalities, the overall structure of the papillae appears largely intact. In stark contrast to this, in the MK6a/b$^{-/-}$ tongues with plaques, the epithelium under the plaque loses all papillar structure and the different cell types lose their characteristic shape. The anterior column cells of MK6a/b$^{-/-}$ tongues with plaques shown in Fig. 4 d were identified based on their keratohyalin granules. The stacking and elongated shape of these cells, however, is completely lost; they are round and much larger than wild-type cells and MK6a/b$^{-/-}$ survivor cells. The MK6a/b$^{-/-}$ tongues with plaques show an abrupt transition between the disorganized epithelium and the plaque material, which suggests that the cells suddenly lose most of their cellular content, whereas the cell envelopes remain attached to each other, forming the plaque. No significant amount of keratohyalin granules was observed in the plaque material. In contrast to this, the wild-type and MK6a/b$^{-/-}$ survivor anterior column cells show the progressive loss of cell organelles towards the outer edge of the papilla with retention of keratohyalin granules in the keratinized squames of the outer layers. This suggests that the build up of the plaque represents a disruption in the terminal differentiation process of the cells due to the loss of structural integrity. The plaque itself appears to consist of cell envelopes and clumps (Fig. 4 d, inset) similar to the ones observed in the anterior column cells of both MK6a/b$^{-/-}$ phenotypes. The clumps most likely consist of keratin proteins since plaque material stains positive for K16 (Fig. 2 k) and K14 (not shown). Somewhat surprisingly, although the posterior column cells also express MK6, and in spite of their slightly disorganized stacking in MK6a/b$^{-/-}$ survivor papillae, their KIF network was apparently normal (not shown). It therefore appears that the presence of MK6 is only essential for the KIF network of the anterior column cells and that the defect in the anterior column cells affects the structure of the entire filiform papilla.

MK6a/b$^{-/-}$ mice reveal the presence of a third MK6 isoform

Since the presence of MK6 appeared to be essential for the structural integrity of the tongue papillae, and the hair follicle and nail bed are two other prominent places of MK6 expression, we were surprised to find that the adult MK6a/b$^{-/-}$ mice showed neither hair nor nail defects. Immunofluorescence analysis of MK6a/b$^{-/-}$ hair follicles and nails, to our amazement, revealed MK6 staining both in the companion cell layer of the MK6a/b$^{-/-}$ hair follicles (Fig. 5 b) and in the dorsal nail beds (Fig. 5 d). The nails of wild-type 4-d-old littermates, in addition to the dorsal staining, also showed MK6 staining on the ventral side (Fig. 5 c), but this became less prominent in nails from 8-d-old pups (not shown). Furthermore, wild-type animals also showed K6 staining in the proximal nail fold, which was not observed in MK6a/b$^{-/-}$ mice (not shown). The MK6 staining in MK6a/b$^{-/-}$ follicles and nails was seen both with an antibody that recognizes MK6a and MK6b (not shown) and with the antibody that reacts with MK6b, but not MK6a (Fig. 5). Since we had confirmed the absence of MK6a and MK6b transcripts in skin by RNase protection analysis, these MK6 antibodies therefore apparently recognize another MK6-like keratin expressed in the hair follicles and nails. However, we detected no MK6 staining in MK6a/b$^{-/-}$ tongue, neither in tongues with plaques nor in survivor tongues, palate, or footpad (data not shown). We therefore suspected that the presence of at least a third K6 gene might explain the absence of follicular and nail defects in these mice. Western blot analysis of day 8 whole skin, using the antibody that recognizes MK6b but not MK6a, revealed a band in the MK6a/b$^{-/-}$ sample that was slightly less intense than the band in the wild-type sample (Fig. 6). Since the level of MK6b mRNA in uninduced skin is very low, it appears likely that MK6a and the

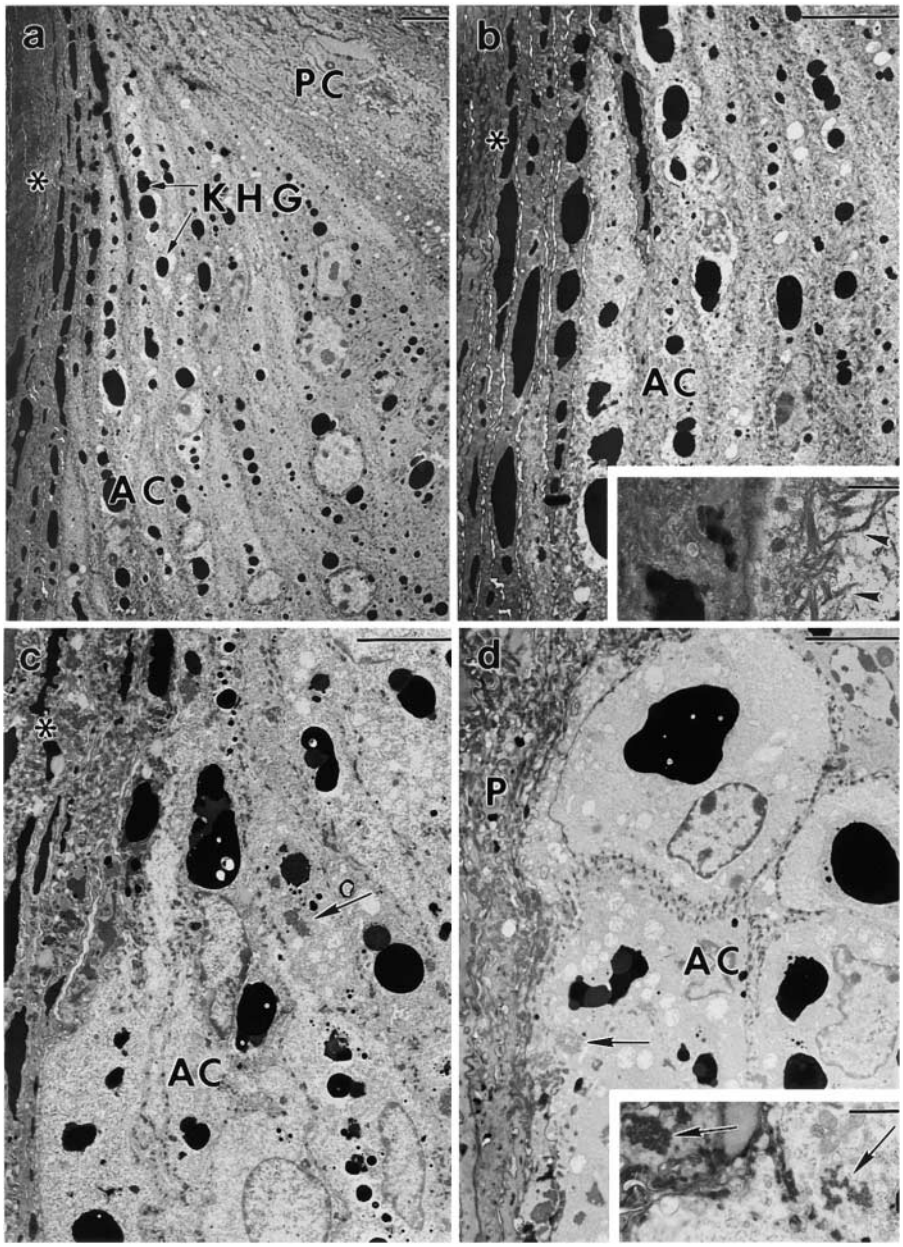

Figure 4. **Electron microscopic comparison of MK6a/b$^{+/+}$ tongues, MK6a/b$^{-/-}$ survivor tongues, and MK6a/b$^{-/-}$ tongues with plaques.** All panels have the same orientation. *Marks the outer keratinized layers of the papilla. (a) Overview of an adult MK6a/b$^{+/+}$ filiform papilla. The anterior column cells (AC) contain keratohyalin granules (KHG), whereas the posterior column (PC) cells do not. (b) Higher magnification of the outer AC shown in a. Note the tight stacking of the cells. The inset shows the prominent KIF bundles (arrowheads) in an anterior column at the boundary to the keratinized layers. The cell shown in the inset was located near the apex of the papilla and is not shown in the larger panel. (c) MK6a/b$^{-/-}$ survivor outer anterior column at the same magnification as b. The cells are not as tightly stacked as the MK6a/b$^{+/+}$ cells and appear not as well aligned with each other. No KIF bundles were seen in the anterior column of MK6a/b$^{-/-}$ survivors; instead, the cells contain apparent keratin clumps (arrow). (d) MK6a/b$^{-/-}$ anterior column under a plaque (P). The cells have completely lost the elongated cell shape and the tight stacking seen in MK6a/b$^{+/+}$ papillae. The cells contain no KIF bundles but apparent keratin clumps (arrow), shown at higher magnification in the inset. (Inset) Keratin clumps in an anterior column (right arrow) and in the plaque (left arrow). Bars: (a–d) 5 μm; (insets in b and d) 1 μm.

third isoform are the predominant isoforms expressed in the hair follicle. MK16 expression was also still present, and if the loading control is taken into account, the amount of MK16 protein appears to be only slightly reduced in the MK6a/b$^{-/-}$ samples.

The third MK6 isoform is orthologous to HK6hf

To clone the third MK6 isoform, we performed a 3′ rapid amplification of cDNA ends (RACE) PCR with RNA isolated from MK6a/b$^{-/-}$ anagen back skin. One PCR product we obtained showed high homology to a human K6 isoform termed HK6hf (for human K6 hair follicle), which is expressed in the companion cell layer of hair follicles, but not in palmar and plantar epidermis or oral epithelia (Winter et al., 1998). We then used the fragment generated by RACE PCR to screen a Stratagene C57BL/6 skin cDNA library and subcloned 10 clones. The four longest clones were selected for sequencing and were found to be identical in their overlapping sequences. Only one clone contained the 5′ end of the gene. Sequence comparison revealed that the mouse clones show 79.8% identity with the HK6hf cDNA (not shown). Conceptual translation of the cDNA gives a protein of 551 amino acids with a calculated molecular mass of 59.7 kD and an isoelectric point of 8.48, which shows 84.8% amino acid identity with the HK6hf protein (Fig. 7). Comparison of the clone with MK6 and MK5 at the cDNA level reveals 74.1% identity with MK6a, 74.7% with MK6b, and 76.6% identity with MK5 (data not shown). At the protein level, the clone has 73.4% identity with MK6a, 72.7% identity with MK6b, and 72.6% identity with MK5 (Fig. 7). Because the clone had higher homology to HK6hf than to the other MK6 isoforms or MK5, and because of its expression pattern, we termed this novel murine keratin MK6hf. To determine whether MK6hf is actually the keratin recognized by our K6 antibodies in the MK6a/b$^{-/-}$ mice, we transfected the full-length MK6hf clone into PtK2 cells. Immunofluo-

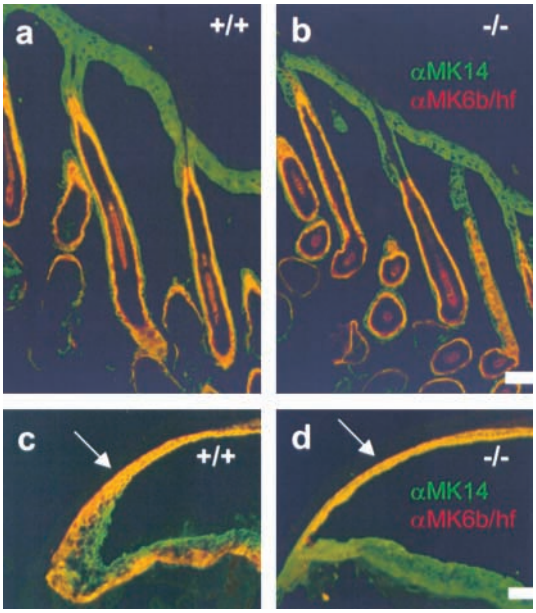

Figure 5. **MK6 staining in the hair follicles and nails of MK6a/b$^{-/-}$ mice.** Sections stained with an MK14 antibody (FITC) and the antibody that recognizes MK6b and MK6hf (Texas red). The overlapping staining appears yellow. (a) MK6a/b$^{+/+}$ back skin from a 4-d-old pup. The companion cell layer of the hair follicles is seen in yellow. (b) MK6a/b$^{-/-}$ back skin from a 4-d-old pup, showing MK6hf staining in the companion cell layer. (c) MK6a/b$^{+/+}$ 4-d-old nail. Note the MK6 staining in the nail bed on the dorsal side of the nail (arrow) as well as on the ventral side. (d) MK6ab$^{-/-}$ 4-d-old nail with MK6 staining in the nail bed (arrow). Bars, 50 μm.

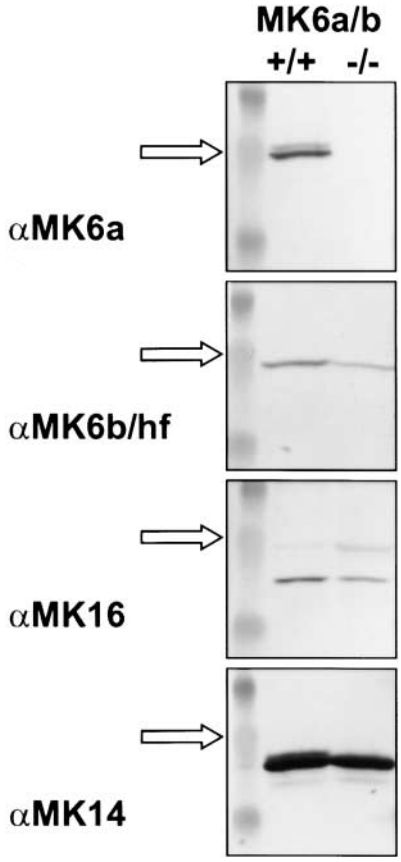

Figure 6. **Western blot analysis of MK6a/b$^{+/+}$ and MK6a/b$^{-/-}$ anagen back skin.** The first lane shows the 84- and 51-kD bands of a protein ladder; the weaker 62.5-kD band is indicated by an arrow. The bands were scanned, and their intensity was measured. Note that the intensity of the MK6b/hf band is reduced by ~50% in the MK6a/b$^{-/-}$ sample, if the loading control (MK14) is taken into account. The MK16 band is also slightly less intense in the MK6a/b$^{-/-}$ sample. Please note that the double bands seen in MK6a and the MK14 are most likely due to differential phosphorylation, whereas the band of higher molecular weight in MK16 may be due to nonspecific reactivity.

rescence analysis confirmed that MK6hf is indeed recognized and, furthermore, that it integrates into the endogenous keratin filament network of these cells (Fig. 8). The expression of MK6hf in the hair follicles and nail beds of MK6a/b$^{-/-}$ mice was additionally confirmed by RT-PCR, using MK6hf specific primers on cDNA samples derived from both total skin and nails (data not shown).

MK6hf is not inducible in response to injury, but MK6a/b$^{-/-}$ full thickness wounds heal without delay

To determine if MK6hf is inducible, we generated full thickness skin wounds in surviving MK6a/b$^{-/-}$ mice. Immunofluorescence analysis of MK6a/b$^{-/-}$ wounded skin using the MK6b/hf antibody revealed that MK6hf is not inducible in the epidermis or ORS, only the constitutive staining in the companion cell layer was seen (Fig. 9 b). The same antibody used on wounded MK6a/b$^{+/+}$ skin showed the suprabasal induction of MK6b in the epidermis (Fig. 9 a). Similarly, no induction was seen in the epidermis using the antibody that recognizes MK6a, MK6b, and MK6hf (not shown). MK6a/b$^{-/-}$ mice still showed induction of MK16 in the epidermis (Fig. 9 b), confirming that MK16 can heterodimerize with another type II partner in both oral mucosa and epidermis. To determine if MK6a/b$^{-/-}$ mice exhibited a defect in the healing of full thickness skin wounds, such wounds were generated in surviving MK6a/b$^{-/-}$ animals, as well as MK6a/b$^{+/+}$ littermates. Animals were killed at 48 h and 5 d after wounding. No significant differences were found in the extent of reepithelialization between MK6a/b$^{-/-}$ and MK6a/b$^{+/+}$ animals at either time point (data not shown). This shows that reepithelialization can occur in the absence of any inducible form of MK6 in the epidermis.

Discussion

Recently, Wong and colleagues (2000) reported the generation of MK6a/b$^{-/-}$ knockout animals that developed oral lesions that lead to starvation and death with 100% penetrance of the phenotype. In contrast, ~25% of our MK6a/b$^{-/-}$ mice from heterozygous intercrosses survived. This divergence between our results and those of Wong and colleagues is most likely due to strain differences; for instance, the 129/SvEv ES cells used by us are distinct from the 129/Sv cells used by Wong et al. (2000). However, the appearance of the tongue lesions that we describe as plaques, including the occurrence of keratin clumps, appears to be very similar to the tongue lesions that Wong and colleagues refer to both as plaques and as blisters. The lack of a nail and hair phenotype in the MK6a/b$^{-/-}$ mice initially seemed surprising; however,

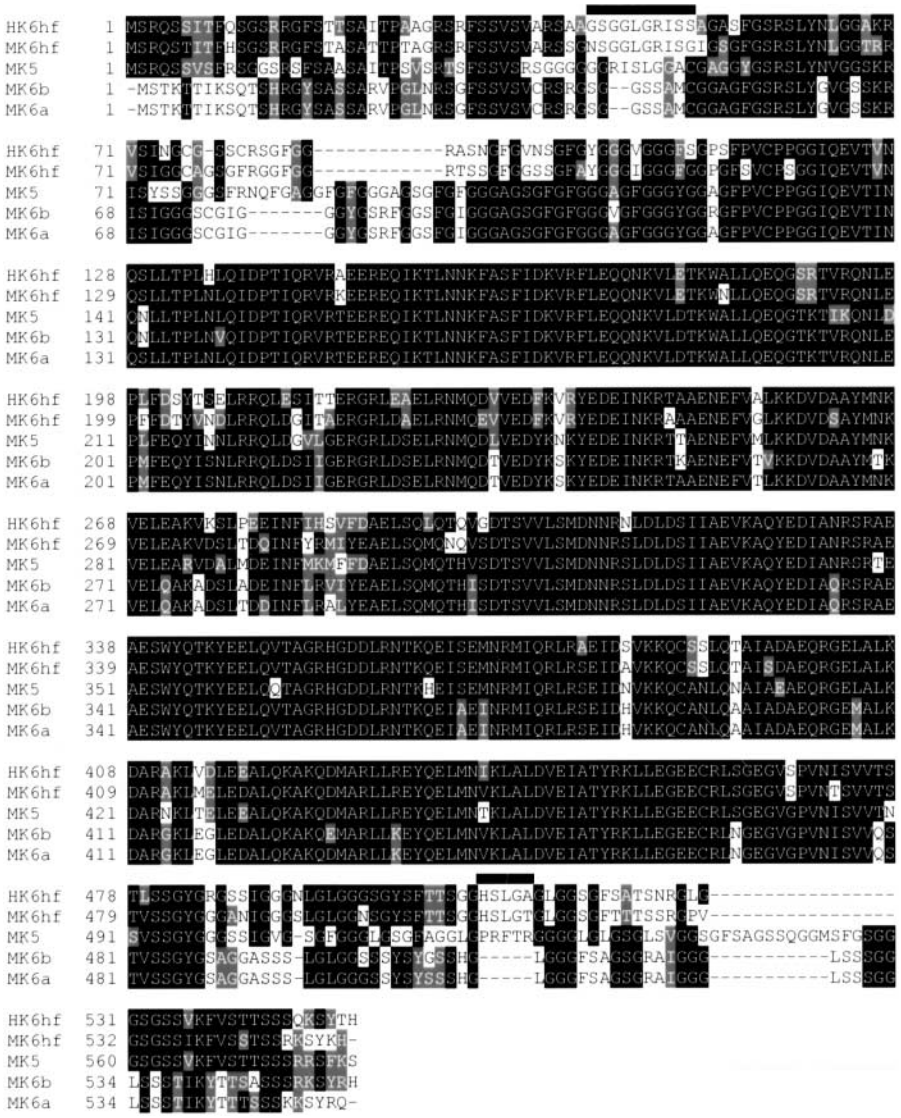

Figure 7. **Alignment of the MK6hf, HK6hf, MK5, MK6a, and MK6b protein sequences.** Identical amino acids are marked by black shading; conservative changes are indicated in gray. The MK6hf protein sequence is more closely related to HK6hf than to MK5, MK6a, or MK6b. Two examples of sections where MK5 differs from MK6a and MK6b are marked by black bars. The sequences of MK6hf and HK6hf in these same regions show stretches of identical amino acids.

our discovery of MK6hf offers an explanation for these unexpected results. Furthermore, the existence of the MK6a/b$^{-/-}$ survivors allowed us to determine that even adult MK6a/b$^{-/-}$ mice have normal nails and hair follicles. This is significant because hair phenotypes in some instances do not become apparent until the completion of the first or even several hair cycles (Koch et al., 1998; Wojcik et al., 1999), and nail defects may also not have time to develop in pups that die before 2 wk of age. Furthermore, we were able to conduct wound healing experiments with the MK6a/b$^{-/-}$ survivors and compare the structural defect discovered in the survivor tongues to MK6a/b$^{-/-}$ tongues with plaques. The conclusions that can be drawn from our findings are discussed below.

The presence of MK6hf offers an explanation for the lack of hair and nail phenotypes in MK6a/b$^{-/-}$ mice

The analysis of our MK6a/b$^{-/-}$ mice uncovered the presence of a third MK6 isoform, which by sequence comparison is the orthologue of HK6hf. The striking discovery of MK6hf expression in hair follicles and nail beds and its absence in tongue suggests that the existence of this new MK6 isoform is the reason for the lack of hair and nail defects in MK6a/b$^{-/-}$ mice. With respect to the expression of MK6a, MK6b, and MK6hf in the companion cell layer, it is interesting to note that this cell layer appears to be particularly sensitive to disruption of its keratin network. We had previously shown that expression of several different MK6a transgenes resulted in the destruction of the companion cells, whereas no alterations were seen in oral epithelia of these transgenic mice (Wojcik et al., 1999). Because the companion cells are thought to provide the slippage plane during the growth of the hair shaft in anagen, the expression of three MK6 isoforms in this compartment may be a safeguard for the maintenance of structural integrity. It therefore seems reasonable to speculate that the deletion of MK6hf, unless there is yet another MK6-like gene, would cause a structural defect in the companion cells and potentially in the nail bed as well. Surprisingly, the MK6a/b$^{-/-}$ mice also have no obvious alterations of their footpads, in spite of the complete absence of K6 expression. However, it is possible that the friction generated on the cage bedding is too insignificant to cause lesions. Furthermore, the periderm of MK6a/b$^{-/-}$ mice also showed an absence of MK6hf expression (data not shown).

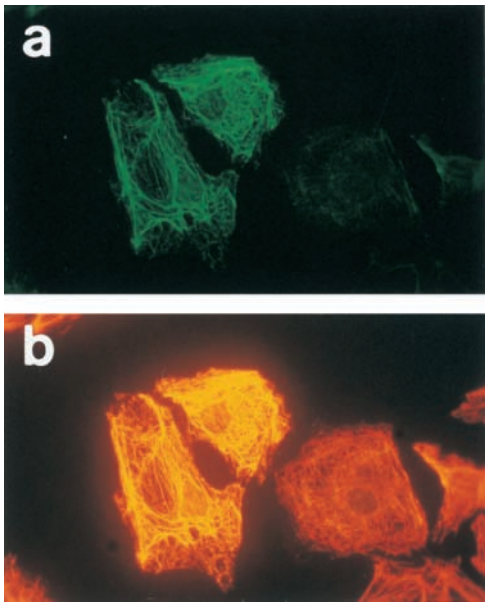

Figure 8. **Transfection of MK6hf into PtK2 cells.** (a) The full-length MK6hf clone encodes a keratin protein that is recognized by the antibody that stains the MK6a/b$^{-/-}$ hair follicle companion cell layer and nail bed (MK6b/hf; FITC). (b) The yellow staining produced by the overlapping staining of MK18 (Texas red), which labels the endogenous keratin network of the cells, and MK6b/hf (FITC) confirms that MK6hf is assembled into the keratin network of the PtK2 cells.

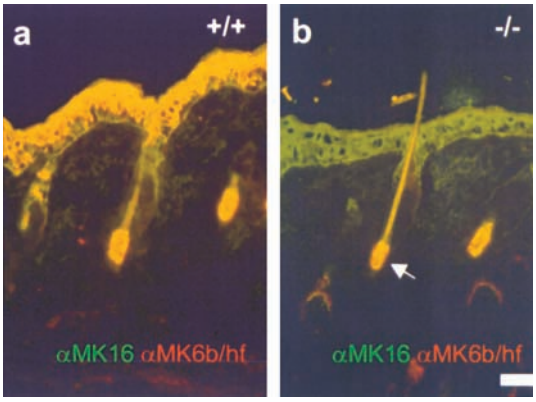

Figure 9. **MK6hf is not inducible in response to wounding.** Both samples were taken from the edge of a 48-h-old full thickness wound and stained with the MK6b/hf antibody (Texas red) and with MK16 (FITC). (a) MK6a/b$^{+/+}$ wound edge. MK16 (FITC) and MK6b (Texas red) induction is seen in the epidermis. Note the suprabasal induction of MK6b (yellow in epidermis). (b) MK6a/b$^{-/-}$ wound edge. MK16 (FITC) is induced, but no induction of MK6hf is seen in the epidermis or in the ORS. Note the MK6hf staining in the companion cell layer (arrow) of the telogen hair follicle. Bar, 50 μm.

It therefore appears that the expression of MK6 in the periderm is not essential for embryonic development. It may be that the role of constitutive K6 expression is one of reinforcement needed only to withstand increased mechanical stress. This hypothesis is supported by the fact that only the back and center of the lingual epithelium, which is subjected to the greatest forces during suckling, deteriorated in the MK6a/b$^{-/-}$ mice.

The white appearance of the plaque on the tongue of MK6a/b$^{-/-}$ animals is reminiscent of the oral leukokeratosis characteristically found in patients with PC-1, caused by dominant-negative mutations in HK6a and HK16. However, the human mutations lead to leukokeratosis of the entire tongue epithelium, but the leukokeratosis does not reach the thickness observed in the MK6a/b$^{-/-}$ mice, nor does it lead to any significant impairment in the patients. Although the MK6a/b$^{-/-}$ phenotype differs from PC-1 in its severity, analogous to the striking heterogeneity found in the tongue phenotype of the MK6a/b$^{-/-}$ mice, some patients with mutations in HK6a or HK16 show no oral involvement (Smith et al., 1999c). Furthermore, there can be considerable variation in the presentation of leukokeratosis within one family (Smith et al., 1999c).

MK6a/b$^{-/-}$ survivors suggest the presence of unknown genetic modifiers

Although the existence of MK6hf may be the explanation for the lack of hair and nail defects in the MK6a/b$^{-/-}$ mice, it does not explain why some of the MK6a/b$^{-/-}$ mice escape death. We observed no MK6 staining in MK6a/b$^{-/-}$ tongues with plaques or in the tongues of survivors. Furthermore, MK6a/b$^{-/-}$ survivor papillae do show microscopically and ultrastructurally observable abnormalities. Most strikingly, keratin clumps identical in appearance were observed in the anterior column cells of survivor tongues and tongues with plaques. Although upregulation of another keratin in the MK6a/b$^{-/-}$ survivors seems the most obvious possibility, the presence of the clumps in both MK6a/b$^{-/-}$ phenotypes argues against this. Since MK6a/b$^{-/-}$ intercrosses produced litters with significantly increased survival rates of between 50% and 100%, the survival seems to be due to genetic modifiers. An even more extreme example of unknown genetic modifiers that affect survival of a keratin knockout are the MK8$^{-/-}$ mice. Deletion of MK8 resulted in midgestational lethality with 94% penetrance in the C57BL/6 background (Baribault et al., 1993), which was rescued in the FVB/N background but, in these mice, caused colorectal hyperplasia in 81% of the mice (Baribault et al., 1994).

A clue to the nature of the rescue in the MK6a/b$^{-/-}$ survivors may lie in the fact that we never observed MK6a/b$^{-/-}$ preweaning pups that were completely free of any sign of a plaque on their tongue. When we killed 1-wk-old MK6a/b$^{-/-}$ pups that showed no sign of starvation, all pups were found to have very small plaques on their tongues. However, all adult MK6a/b$^{-/-}$ survivor tongues were macroscopically normal. This strongly suggests that MK6a/b$^{-/-}$ survivors develop plaques on their tongues as pups and that these plaques later resolve and the lingual epithelium recovers, leaving only the mild structural abnormalities found in the adult survivors. The modifiers that affect the survival of the MK6a/b$^{-/-}$ mice may influence the degree to which the plaque develops rather than whether it forms at all; one possibility would be that they affect the hyperplastic response to the structural defect. If this hypothesis is correct, K6 is indeed essential to the structural integrity of the lingual epithelium; however, this is only of critical importance during the time the animals are suckling. Once the animals switch to chewing solid food, the forces that the epithelium has to withstand should be less than what is needed to create the suction necessary for suckling. The increased proliferation

rates observed in the MK6a/b$^{-/-}$ survivor tongues, along with the mild structural abnormalities, suggest a narrowly maintained balance of epithelial integrity in these animals. The genetic modifiers that affect this balance could potentially be found through backcrosses into different strains and may offer further insight into the factors that control epithelial proliferation in response to injury.

Implications for the role of MK6 in wound healing

Since MK6a/b$^{-/-}$ mice lack any inducible K6 but are nonetheless able to reepithelialize full thickness wounds without any obvious delay, it appears that the role of K6 induction in wound healing is fairly subtle. We had previously shown that MK6a$^{-/-}$ mice exhibited a delay in the reepithelialization of superficial wounds from the hair follicles, but were indistinguishable from wild-type animals in the healing of full thickness wounds. Although the analysis of MK6a$^{-/-}$ full thickness wounds had already indicated that the proliferating and migrating cells in the MK6a$^{-/-}$ full thickness wounds did not express any MK6 (Wojcik et al., 2000), we could not entirely exclude that the lack of a defect in full thickness wound healing was due to the presence of MK6b in the suprabasal layers in the newly forming epithelium. The absence of an obvious defect in the healing of full thickness wounds in MK6a/b$^{-/-}$ mice now confirms that MK6 induction does not play a prominent role in the progression of reepithelialization in these types of wounds.

At this point, we have not been able to investigate the healing of superficial wounds in the MK6a/b$^{-/-}$ mice, due to the large number of animals needed for this experiment. Since neither MK6a$^{-/-}$ nor MK6a/b$^{-/-}$ mice showed any defect in the healing of full thickness wounds, it may be that the delay in seen in MK6a$^{-/-}$ superficial wound healing is specific to the follicular keratinocytes. This leaves open the question of what the function of MK6a and MK6b induction in the newly forming epithelium covering the wound might be. There are several possible explanations, which are not mutually exclusive. First, K16 was still induced in the MK6a/b$^{-/-}$ wounds. If the induction of K6 and K16 results in changes in the properties of the keratinocyte IF network that allow for greater flexibility needed for migration, K16 induction alone may be sufficient to effect those IF network changes, as has indeed been previously suggested for HK16 (Paladini et al., 1996). However, results obtained with MK16 do not support this scenario (Porter et al., 1998). Second, the main function of K6 induction in wounded epithelium may be one of structural reinforcement. One feature that the epithelia that express K6 have in common may be a need for added mechanical strength. The companion cell layer is subject to friction, as are footpads, and oral epithelia. Like the tongue epithelium during suckling, the epithelium covering a wound in which the dermis was damaged could be expected to require greater mechanical strength than intact epidermis. The characteristic inducible expression of K6 may therefore essentially serve the same function as its constitutive expression: to provide additional structural support in areas that have to withstand increased mechanical stress. In that sense, the link between K6 induction and hyperproliferating cells may serve the purpose to place K6 expression at the wound site for added structural support rather than be of great importance to the proliferation or migration process of the cells. This hypothesis might be difficult to test experimentally, but if a humane and reproducible way to exert friction on MK6a/b$^{-/-}$ and wild-type wounds with scabs could be devised, such an experiment might answer the question of why K6 is induced in response to wounding.

Materials and methods

Construction of the MK6a/b targeting vector

The 5′ arm of the MK6a/b targeting vector was identical to the 5′ arm of the vector used to generate MK6a$^{-/-}$ mice, and its cloning and ligation to the selection cassette containing the hypoxanthine phosphoribosyl transferase minigene and a neomycin cassette (hprtΔ3′-neo) has been previously described (Wojcik et al., 2000). The hprtΔ3′-neo cassette was provided by Allan Bradley (Baylor College of Medicine, Houston, TX). For a more detailed description of the underlying targeting strategy, see Ramirez-Solis et al. (1995). For the construction of the MK6a/b targeting vector a 7 kb SacI-SphI fragment directly downstream of the MK6b stop codon was subcloned into pGEM3zf (Promega). A 3.2-kb XbaI-HindIII fragment that begins 0.26 kb downstream of the MK6b stop codon was used as the 3′ arm. To construct the MK6a/b targeting vector, the following four fragments were simultaneously ligated: the 9.7-kb SalI-NotI fragment with the 5 kb 5′ arm and the hprtΔ3′-neo cassette, a 3.2-kb NotI-BamHI fragment of the MK6b flanking region, a 2.1-kb BamHI-HindIII fragment containing the thymidine kinase cassette (provided by John Lydon, Baylor College of Medicine), and the 2.74-kb pGEM3z backbone cut with HindIII and SalI. Before electroporation, the MK6a/b targeting vector was linearized with SalI.

Generation of MK6a/b-deficient mice

ES cells (AB2.2, 129/SvEv) and feeder cells SNL76/7 (McMahon and Bradley, 1990) were provided by Allan Bradley. Cell culture, drug selection, expansion of clones on 96 well plates, and Southern screening of clonal DNA were performed according to published protocols (Ramirez-Solis et al., 1992, 1993). To screen the 5′ end of the targeted locus, DNA for Southern analysis was digested with EcoRV and probed with a 0.9-kb BglII-SalI fragment that lies just outside the 5′ arm of the targeting vector (Fig. 1 a). To confirm the 3′ end of the MK6a/b targeted locus, ES cell DNA was digested with SphI, and the Southern blots were probed with an external 0.7-kb KpnI-PstI fragment.

Genotyping of mice

DNA for genotyping was prepared from tail biopsies. Litters from MK6a/b$^{+/-}$ intercrosses were screened using primers 5′-AGATCCACTAGTTCTAGCCTCG-3′, 5′-AGAGATGGCATCATGTGAGC-3′, and 5′-GGAAGAGCTACAGGCACTGA-3′.

Animal protocols

Mice were kept under standard housing conditions at the animal facility at Baylor College of Medicine. Wound healing protocols were approved by the Center for Comparative Medicine. Mice were anesthetized using 0.0175 ml of 2.5% avertin per gram mouse. For the duration of each wound healing experiment, acetaminophen (Children's Tylenol) was added to the drinking water at 1 mg/ml, and sulfamethoxazole/trimethoprim oral suspension (Apothecon) was added at 1 ml/150 ml. Full thickness wounds were generated in the center of the lower back after shaving and wiping with betadine solution. A circle of 5 mm diameter was marked on the skin and excised using curved scissors. Reepithelialization of full thickness wounds was assessed according to the length of the epithelial tongues migrating from the edge of the wounds. In vivo BrdU labeling of tongues was carried out by intraperitoneal injection of 0.01 ml of 10 mg/ml BrdU-triphosphate (Sigma-Aldrich) per gram mouse. Mice were killed 1.5 h after the BrdU injection. The tongues were imbedded in OCT, and immunostaining was done as described below.

RNA isolation and RNase protection analysis

Total RNA was isolated from whole anagen back skin with RNAzol B (Tel-Test). The RNA probe for MK6 was designed to protect 382 bases in MK6a and 268 bases in MK6b but does not detect MK6hf. The generation of the probe has been previously described (Wojcik et al., 2000). RNA probes for MK6a/b and cyclophilin (Ambion) were generated using α[^{32}P]CTP and the Riboprobe Gemini II kit (Promega). Probes were purified on 5% acryl-

amide gels before the hybridization. The RNase protection assay was performed with the RPA II kit (Ambion) with overnight hybridization at 42°C.

Western blot analysis

Tissue samples were ground in liquid N_2 and then solubilized in loading buffer, electrophoresed, and blotted onto nitrocellulose as previously described (Bickenbach et al., 1996). Blots were blocked with 5% nonfat milk-TBS and then probed with rabbit anti-K6, sheep anti-K14 (Roop et al., 1984), guinea pig anti-K6 (Rothnagel et al., 1999), and rabbit anti-K16 (Porter et al., 1998), followed by alkaline phosphatase–conjugated anti–rabbit IgG (Boehringer), anti–guinea pig IgG (Zymed Laboratories), and anti–sheep IgG (Zymed Laboratories), respectively. Bands were visualized using nitroblue tetrazolium/5-bromo-4-chloro-3-indolylphosphate solution (Boehringer) according to the manufacturer's instructions. The blots were photographed and scanned, and the intensity was measured using QuantiScan v1.5 (Biosoft).

Processing of tissue samples

For histological analysis, pieces of tissue were fixed overnight in Carnoys' solution (ethanol/chloroform/glacial acetic acid, 6:3:1), processed for paraffin embedding, and sectioned at 5–6 μm. The sections were deparaffinized and stained with hematoxylin and eosin. Immunofluorescence analysis was done on unfixed frozen sections. Samples for frozen sections were imbedded in Tissue Tek® OCT compound (Sakura Finetek). The frozen blocks were sectioned at 5–6 μm. Frozen sections were washed twice for 10 min in PBS before incubation with the appropriate antibodies. BrdU-labeled samples were incubated first for 10 min in PBS and then for 12.5 min in 25% HCl and finally rinsed three times for 10 min in PBS before incubation with the antibodies.

Double-label immunofluorescence

Two-color immunofluorescence was performed by sequential incubation with primary antibodies and FITC- or Texas red–conjugated secondary antibodies. Primary antibodies used were rabbit anti-MK6, rabbit anti-MK14, guinea pig anti-MK14 (Roop et al., 1984), and rabbit anti-MK16 (Porter et al., 1998). Furthermore, a guinea pig anti-HK6 antibody (Rothnagel et al., 1999), which in mouse recognizes MK6b (Rothnagel et al., 1994, 1999) and MK6hf, and a mouse monoclonal anti-K18 antibody (Sigma-Aldrich) were used. Incubation with primary antibodies was done overnight at 4°C. Secondary antibody conjugates used were FITC-conjugated anti–rabbit (Dako), Texas red–conjugated anti–guinea pig (Vector Laboratories), FITC-conjugated anti–guinea pig (Zymed Laboratories) as well as biotinylated anti–mouse (Vector Laboratories) followed by Texas red–conjugated streptavidin (GIBCO BRL). Incubation with secondary antibodies was done at room temperature for 30 min. For BrdU-labeled samples, the primary keratin antibody was diluted into the FITC-conjugated anti-BrdU (Becton Dickinson) followed by a second incubation with Texas red–conjugated anti–guinea pig (Vector Laboratories).

Electron microscopy

For electron microscopy, tissue samples were fixed with 2.5% glutaraldehyde in 0.1 M cacodylate buffer (pH 7.3), embedded in epon, sectioned, and then stained with lead citrate and aqueous uranyl acetate. The samples were viewed at 75 kV using a Hitachi H7000 transmission electron microscope.

Cloning of MK6hf

RNA was isolated from MK6a/b$^{-/-}$ anagen back skin as described above. The 3′ RACE was performed using the SMART™ RACE cDNA amplification kit (CLONTECH Laboratories, Inc.) with PowerSript™ reverse transcriptase (CLONTECH Laboratories, Inc.) under the conditions suggested by the manufacturer. The primer used with the kit was 5′-CCACCTACAGGAAGCTGCTGGA-3′, which anneals to a region corresponding to the TYRLEGEE sequence at the COOH terminus of the rod domain of all keratins, and in combination with the kit's primer to the polyA tail, the 3′ ends of multiple keratin cDNAs present in the MK6a/b$^{-/-}$ skin sample were amplified. Since amplification of MK6a and MK6b would produce fragments of ~860 bp, two fragments of ~750 and ~900 bp were subcloned into pGEM-T (Promega) and sequenced. BLAST searches using the WWW Blast interface, revealed that the larger fragment showed high homology to HK6hf (Winter et al., 1998). This fragment was then used as a probe to screen an 11-wk old mouse skin C57BL/6 Uni-ZAP® XR Library (Stratagene) according to the manufacturer's instructions. 10 clones were selected, and the inserts in the pBluescript SK phagemid were excised from the Uni-ZAP XR Vector according to the manufacturer's protocol. The four longest clones were sequenced and were found to be identical, one clone containing the apparently full-length MK6hf cDNA. The MK6hf cDNA sequence was assembled from the overlapping sequencing results of all four clones. DNA sequence analysis and conceptual translation was done using GCG (Wisconsin Package v10.0, Genetics Computer Group). Alignments of protein sequences were done with the ClustalW v1.8 WWW interface, and the shading was done using the WWW boxshade server. For transfection of MK6hf, the full-length MK6hf clone was excised from the pBluescript vector with EcoRI and XhoI and directly cloned into the pcDNA3.1(+) expression vector (Invitrogen).

Cell culture and transfection of MK6hf

PtK2 cells, a rat kangaroo kidney epithelial cell line, were cultured in EMEM (GIBCO BRL) with 10% fetal bovine serum and 1.26 mM Ca^{2+}. Cells were plated at a density of 0.5×10^5 cells per cm^2 on 50 mm^2 glass cover slips in six-well dishes. The full-length MK6hf clone, subcloned into the pcDNA3.1(+) expression vector (Invitrogen), was used for transfections. The cells were transfected 24 h after plating (at ~60% confluency) using the TransIT-LT1 reagent (Panvera) in the complete growth medium according to the manufacturer's instructions. The cells were allowed to grow for 40 h after transfection and then fixed for 5 min in cold methanol/acetone (1:1), followed by 5 min in 70% ethanol, and stained using the antibody that recognizes MK6b and MK6hf and a mouse monoclonal anti-K18 antibody (Sigma-Aldrich). Untransfected cells were used as a negative control.

The authors would like to thank Hank Adams for electron microscopy and Rebecca Porter and E. Brigitte Lane (University of Dundee, Dundee, UK) for providing the anti-MK16 antibody. We would like to give special thanks to Peter Koch for technical suggestions and comments on the manuscript.

This work was supported by National Institutes of Health grant HD25479 to D.R. Roop.

Submitted: 15 February 2001
Revised: 29 June 2001
Accepted: 29 June 2001

References

Baribault, H., J. Price, K. Miyai, and R.G. Oshima. 1993. Mid-gestational lethality in mice lacking keratin 8. *Genes Dev.* 7:1191–1202.

Baribault, H., J. Penner, R.V. Iozzo, and M. Wilson-Heiner. 1994. Colorectal hyperplasia and inflammation in keratin 8-deficient FVB/N mice. *Genes Dev.* 8:2964–2973.

Bickenbach, J.R., M.A. Longley, D.S. Bundman, A.M. Dominey, P.E. Bowden, J.A. Rothnagel, and D.R. Roop. 1996. A transgenic mouse model that recapitulates the clinical features of both neonatal and adult forms of the skin disease epidermolytic hyperkeratosis. *Differentiation*. 61:129–139.

Blessing, M., H. Zentgraf, and J.L. Jorcano. 1987. Differentially expressed bovine cytokeratin genes. Analysis of gene linkage and evolutionary conservation of 5′-upstream sequences. *EMBO J.* 6:567–575.

Bowden, P.E., J.L. Haley, A. Kansky, J.A. Rothnagel, D.O. Jones, and R.J. Turner. 1995. Mutation of a type II keratin gene (K6a) in pachyonychia congenita. *Nat. Genet.* 10:363–365.

Celebi, J.T., E.L. Tanzi, Y.J. Yao, E.J. Michael, and M. Peacocke. 1999. Mutation report: identification of a germline mutation in keratin 17 in a family with pachyonychia congenita type 2. *J. Invest. Dermatol.* 113:848–850.

Corden, L.D., and W.H. McLean. 1996. Human keratin diseases: hereditary fragility of specific epithelial tissues. *Exp. Dermatol.* 5:297–307.

Covello, S.P., F.J. Smith, J.H. Sillevis-Smith, A.S. Paller, C.S. Munro, M.F. Jonkman, J. Uitto, W.H. McLean. 1998. Keratin 17 mutations cause either steatocystoma multiplex or pachyonychia congenita type 2. *Br. J. Dermatol.* 139:475–480.

Fujimoto, W., G. Nakanishi, S. Hirakawa, T. Nakanishi, T. Shimo, M. Takigawa, and J. Arata. 1998. Pachyonychia congenita type 2: keratin 17 mutation in a Japanese case. *J. Am. Acad. Dermatol.* 38:1007–1009.

Hatzfeld, M., and K. Weber. 1990. The coiled coil of in vitro assembled keratin filaments is a heterodimer of type I and II keratins: use of site-specific mutagenesis and recombinant protein expression. *J. Cell Biol.* 110:1199–1210.

Ito, M. 1986. The innermost cell layer of the outer root sheath in anagen hair follicle: light and electron microscopic study. *Arch. Dermatol. Res.* 279:112–119.

Ito, M. 1988. Electron microscopic study on cell differentiation in anagen hair follicles in mice. *J. Invest. Dermatol.* 90:65–72.

Iwasaki, S., Y. Okumura, and M. Kumakura. 1999. Ultrastructural study of the relationship between the morphogenesis of filiform papillae and the keratiniza-

tion of the lingual epithelium in the mouse. *Cells Tissues Organs.* 165:91–103.

Jiang, C.K., T. Magnaldo, M. Ohtsuki, I.M. Freedberg, F. Bernerd, and M. Blumenberg. 1993. Epidermal growth factor and transforming growth factor α specifically induce the activation- and hyperproliferation-associated keratins 6 and 16. *Proc. Natl. Acad. Sci. USA.* 90:6786–6790.

Kao, W.W., C.Y. Liu, R.L. Converse, A. Shiraishi, C.W. Kao, M. Ishizaki, T. Doetschman, and J. Duffy. 1996. Keratin 12-deficient mice have fragile corneal epithelia. *Invest. Ophthalmol. Vis. Sci.* 37:2572–2584.

Koch, P.J., M.G. Mahoney, G. Cotsarelis, K. Rothenberger, R.M. Lavker, and J.R. Stanley. 1998. Desmoglein 3 anchors telogen hair in the follicle. *J. Cell Sci.* 111:2529–2537.

Leigh, I.M., H. Navsaria, P.E. Purkis, I.A. McKay, P.E. Bowden, and P.N. Riddle. 1995. Keratins (K16 and K17) as markers of keratinocyte hyperproliferation in psoriasis in vivo and in vitro. *Br. J. Dermatol.* 133:501–511.

Lloyd, C., Q.C. Yu, J. Cheng, K. Turksen, L. Degenstein, E. Hutton, and E. Fuchs. 1995. The basal keratin network of stratified squamous epithelia: defining K15 function in the absence of K14. *J. Cell Biol.* 129:1329–1344.

McLean, W.H., E.L. Rugg, D.P. Lunny, S.M. Morley, E.B. Lane, O. Swensson, P.J. Dopping-Hepenstal, W.A. Griffiths, R.A. Eady, and C. Higgins. 1995. Keratin 16 and keratin 17 mutations cause pachyonychia congenita. *Nat. Genet.* 9:273–278.

McMahon, A.P., and A. Bradley. 1990. The Wnt-1 (int-1) proto-oncogene is required for development of a large region of the mouse brain. *Cell.* 62:1073–1085.

Navarro, J.M., J. Casatorres, and J.L. Jorcano. 1995. Elements controlling the expression and induction of the skin hyperproliferation-associated keratin K6. *J. Biol. Chem.* 270:21362–21367.

Ness, S.L., W. Edelmann, T.D. Jenkins, W. Liedtke, A.K. Rustgi, and R. Kucherlapati. 1998. Mouse keratin 4 is necessary for internal epithelial integrity. *J. Biol. Chem.* 273:23904–23911.

Orwin, D.F. 1971. Cell differentiation in the lower outer sheath of the Romney wool follicle: a companion cell layer. *Aust. J. Biol. Sci.* 24:989–999.

Paladini, R.D., K. Takahashi, N.S. Bravo, and P.A. Coulombe. 1996. Onset of reepithelialization after skin injury correlates with a reorganization of keratin filaments in wound edge keratinocytes: defining a potential role for keratin 16. *J. Cell Biol.* 132:381–397.

Paulson, R.B., T.G. Hayes, and M.E. Sucheston. 1985. Scanning electron microscope study of tongue development in the CD-1 mouse fetus. *J. Craniofac. Genet. Dev. Biol.* 5:59–73.

Porter, R.M., S. Leitgeb, D.W. Melton, O. Swensson, R.A. Eady, and T.M. Magin. 1996. Gene targeting at the mouse cytokeratin 10 locus: severe skin fragility and changes of cytokeratin expression in the epidermis. *J. Cell Biol.* 132:925–936.

Porter, R.M., A.M. Hutcheson, E.L. Rugg, R.A. Quinlan, and E.B. Lane. 1998. cDNA cloning, expression, and assembly characteristics of mouse keratin 16. *J. Biol. Chem.* 273:32265–32272.

Ramirez-Solis, R., J. Rivera-Perez, J.D. Wallace, M. Wims, H. Zheng, and A. Bradley. 1992. Genomic DNA microextraction: a method to screen numerous samples. *Anal. Biochem.* 201:331–335.

Ramirez-Solis, R., A.C. Davis, and A. Bradley. 1993. Gene targeting in embryonic stem cells. *Methods Enzymol.* 225:855–878.

Ramirez-Solis, R., P. Liu, and A. Bradley. 1995. Chromosome engineering in mice. *Nature.* 378:720–724.

Roop, D.R., C.K. Cheng, L. Titterington, C.A. Meyers, J.R. Stanley, P.M. Steinert, and S.H. Yuspa. 1984. Synthetic peptides corresponding to keratin subunits elicit highly specific antibodies. *J. Biol. Chem.* 259:8037–8040.

Rothnagel, J.A., H. Traupe, S. Wojcik, M. Huber, D. Hohl, M.R. Pittelkow, H. Saeki, Y. Ishibashi, and D.R. Roop. 1994. Mutations in the rod domain of keratin 2e in patients with ichthyosis bullosa of Siemens. *Nat. Genet.* 7:485–490.

Rothnagel, J.A., T. Seki, M. Ogo, M.A. Longley, S.M. Wojcik, D.S. Bundman, J.R. Bickenbach, and D.R. Roop. 1999. The mouse keratin 6 isoforms are differentially expressed in the hair follicle, footpad, tongue and activated epidermis. *Differentiation.* 65:119–130.

Shamsher, M.K., H.A. Navsaria, H.P. Stevens, R.C. Ratnavel, P.E. Purkis, D.P. Kelsell, W.H. McLean, L.J. Cook, W.A. Griffiths, and S. Gschmeissner. 1995. Novel mutations in keratin 16 gene underly focal non-epidermolytic palmoplantar keratoderma (NEPPK) in two families. *Hum. Mol. Genet.* 4:1875–1881.

Smith, F.D., M.F. Jonkman, H. Vangoor, C.M. Coleman, S.P. Covello, J. Uitto, and W.I. Mclean. 1998. A mutation in human keratin K6b produces a phenocopy of the K17 disorder pachyonychia congenita type 2. *Hum. Mol. Genet.* 7:1143–1148.

Smith, F.J., M. Del Monaco, P.M. Steijlen, C.S. Munro, M. Morvay, C.M. Coleman, F.J. Rietveld, J. Uitto, and W.H. McLean. 1999a. Novel proline substitution mutations in keratin 16 in two cases of pachyonychia congenita type 1. *Br. J. Dermatol.* 141:1010–1016.

Smith, F.J., K.E. McKenna, A.D. Irvine, E.A. Bingham, C.M. Coleman, J. Uitto, and W.H. McLean. 1999b. A mutation detection strategy for the human keratin 6A gene and novel missense mutations in two cases of pachyonychia congenita type 1. *Exp. Dermatol.* 8:109–114.

Smith, F.J., V.A. McKusick, K. Nielsen, E. Pfendner, J. Uitto, and W.H. McLean. 1999c. Cloning of multiple keratin 16 genes facilitates prenatal diagnosis of pachyonychia congenita type 1. *Prenat. Diagn.* 19:941–946.

Steinert, P.M. 1990. The two-chain coiled-coil molecule of native epidermal keratin intermediate filaments is a type I-type II heterodimer. *J. Biol. Chem.* 265: 8766–8774.

Takahashi, K., R.D. Paladini, and P.A. Coulombe. 1995. Cloning and characterization of multiple human genes and cDNAs encoding highly related type II keratin 6 isoforms. *J. Biol. Chem.* 270:18581–18592.

Takahashi, K., B. Yan, K. Yamanishi, S. Imamura, and P.A. Coulombe. 1998. The two functional keratin 6 genes of mouse are differentially regulated and evolved independently from their human orthologs. *Genomics.* 53:170–183.

Winter, H., L. Langbein, S. Praetzel, M. Jacobs, M.A. Rogers, I.M. Leigh, N. Tidman, and J. Schweizer. 1998. A novel human type II cytokeratin, K6hf, specifically expressed in the companion layer of the hair follicle. *J. Invest. Dermatol.* 111:955–962.

Wojcik, S.M., S. Imakado, T. Seki, M.A. Longley, L. Petherbridge, D.S. Bundman, J.R. Bickenbach, J.A. Rothnagel, and D.R. Roop. 1999. Expression of MK6a dominant-negative and C-terminal mutant transgenes in mice has distinct phenotypic consequences in the epidermis and hair follicle. *Differentiation.* 65:97–112.

Wojcik, S.M., D.S. Bundman, and D.R. Roop. 2000. Delayed wound healing in keratin 6a knockout mice. *Mol. Cell. Biol.* 20:5248–5255.

Wong, P., E. Colucci-Guyon, K. Takahashi, C. Gu, C. Babinet, and P.A. Coulombe. 2000. Introducing a null mutation in the mouse K6α and K6β genes reveals their essential structural role in the oral mucosa. *J. Cell Biol.* 150: 921–928.